OPEN FILE REPORT 1985-4

##

SILICA TRANSPORT DURING STEAM INJECTION INTO OIL SANDS: I. DISSOLUTION AND PRECIPITATION KINETICS OF QUARTZ — NEW RESULTS AND REVIEW OF EXISTING DATA.

##

G. Bird and J. Boon

Oil Sands Research Department
Alberta Research Council
Edmonton, Alberta, Canada

February 1984

File No. 1545-1-18

ABSTRACT

The literature on quartz and silicate dissolution kinetics is briefly reviewed. Fifteen dissolution and seven precipitation experiments with time as the independent variable, and four dissolution experiments with the ratio A/M (surface area of sand)/mass of water) as the independent variable are described. The experiments were carried out at temperatures between 121 and 255°C. Oil sand from which the bitumen had been previously extracted was used in all dissolution experiment. Both parabolic and first order rate laws could be fitted to the data. The use of either rate law leads to an activation energy for precipitation in the range 51-55 kJ $mole^{-1}$. Depending on the way an experiment is conducted, the ratio A/M may affect the results. The first order rate law is useful for predicting silica mass transport during steam injection.

1. INTRODUCTION

The in situ exploitation of many deeply buried heavy oil and tar sands deposits involves the injection of large volumes of hot water or steam into quartz rich sedimentary formations at pressures up to 12 MPa and temperatures up to 325°C.

The solubility of silica minerals in water is determined primarily by temperature and pH with ionic strength and pressure being of secondary importance under these conditions. Hot injection fluids react rapidly with quartz and substantial mass transport of silica must occur. Gravel pack disintegration and well collapse have been recorded (Reed, 1979). The injected fluids probably become saturated with respect to quartz and other salts at a short distance from the injection well. As this water continues to move outward into the formation it cools and silica can precipitate, either as amorphous silica or as quartz. It can also react with other dissolved mineral components to produce new mineral phases. The rate of silica precipitation or reaction will determine where in the formation precipitation occurs and how it affects reservoir properties. McCorriston et al. (1981) have shown that such reaction can lead to significant irreversible changes in permeability.

We undertook our study to obtain data that can be used to predict the extent of quartz dissolution and precipitation around injection and production well bores and to derive and refine the rate equations needed in silica mass transport. In this paper we are reporting twenty-seven new experimental measurements on appropriate oil sand and quartz sand systems and reviewing the existing literature data on quartz dissolution and precipitation. In the second paper in this series we will use this information to estimate the amount of silica transport during in situ exploitation of heavy oil resources.

2. THEORY

The quartz dissolution reaction is generally written as:

$$SiO_2 + 2\ H_2O = H_4SiO_4 \qquad (1)$$

At pH greater than 8, ionization of silicic acid becomes important:

$$H_4SiO_4 + OH^- = H_3SiO_4^- + H_2O \qquad (2)$$

and quartz solubility greatly increases with pH.

The solubility of quartz has been studied extensively and several reviews of the existing data have been published (Crerar and Anderson, 1971; Walther and Helgeson, 1977; Rimstidt, 1979; Fournier and Potter, 1982; and Fleming and Crerar, 1982). The solubility of quartz in vapor-saturated liquid water can be described by the equation:

$$\text{Log } K_{eq} = 3.3105 + \frac{252.93}{T} - \frac{3.2168}{T^2} \times 10^5 \qquad (3)$$

where T is expressed in degrees Kelvin and K_{eq} in parts per million SiO_2 (Crerar and Anderson, 1971).

It has been generally assumed that the dissolution rate of quartz is controlled by a zero order surface reaction (Equation 4) and that its precipitation rate is first order (Equation 5) (van Lier, 1960; Rimstidt, 1979, Rimstidt and Barnes 1980).

$$\left(\frac{dC}{dt}\right)_{forward} = k_+(A/M) \qquad (4)$$

where

C = silica concentration (mass fraction)

t = time

k_+ = forward rate constant

A = surface area of the sample

M = mass of water

and

$$\left(\frac{dC}{dt}\right)_{\text{backward}} = -k_-C(A/M) \tag{5}$$

where k_- = backward rate constant.

The net rate of concentration change is

$$\frac{dC}{dt} = (k_+ - k_-C)(A/M) \tag{6}$$

Assuming unit activity of water and unit activity coefficient of dissolved silica and using $\frac{dC}{dt} = 0$ at equilibrium, Equation (6) can be rearranged to give:

$$\frac{k^+}{k_-} = K_{eq} = C_{eq} \tag{7}$$

where C_{eq} = equilibrium concentration.

From (6) and (7):

$$\frac{dC}{dt} = k_-(A/M)\ (C_{eq}-C) \tag{8}$$

Integration of (8) gives:

$$\ln \left[\frac{1-C/C_{eq}}{1-Co/C_{eq}} \right] = -k_{-}(A/M)t. \qquad (9)$$

where C_o = silica concentration at t = 0. If C_o = 0, equation (9) reduces to:

$$\ln [1-C/C_{eq}] = -k_{-}(A/M)t \qquad (10)$$

It is convenient to express all results relative to a reference system of constant surface area and mass of water. We chose the same reference system as Rimstidt (1979) and Rimstidt and Barnes (1980): surface area 1 m^2, mass of water 1 kg. Therefore in this paper k_{-} has the dimension sec^{-1}.

It is also possible to develop other rate equations of a theoretical or empirical nature to describe the rate of change of concentration in solution. Helgeson (1971) developed a rate equation of the form:

$$\frac{dC_i}{dt} = k_i \, t^{\omega} \qquad (11)$$

to describe silicate dissolution rates. This derivation assumed that the reaction rate was partially controlled by the rate of diffusion of reactants through a porous reaction layer of variable thickness. In this model ω varied with time and could have values of 0, -1 and -1/2, in which case the equation took the form of a linear, logarithmic or parabolic rate law respectively. Although a number of silicate dissolution reactions have been shown to follow this rate law (Wollast, 1967; Lagache, 1976; Petrovic, 1976; Fung et al., 1980; and others) the diffusion control mechanism on which the equation is based has been refuted as no evidence has been forthcoming to show the presence of a porous reaction zone (see discussion in

Aagard and Helgeson, 1982). Dibble and Tiller (1981) proposed a model for interface-controlled dissolution reactions in which a molecule is transferred from solid to solution through a sequence of distinct steps. The driving energy for dissolution, which is related to the undersaturation of the bulk solution can be partially consumed by processes other than surface detachment. Dibble and Tiller assumed that diffusion through the fluid is rapid relative to surface detachment and showed that both linear or logarithmic kinetics are possible, depending on the mechanism that dominates the surface reaction.

The logarithmic rate equation that Dibble and Tiller derived is similar in form to equation (10). It was concluded that a parabolic rate law was possible only if one or more of the surface detachment parameters vary with time. Unfortunately, published data that can be used to quantify any of the particular mechanisms that cause the rate law to vary with time are not available.

Aagard and Helgeson (1982) developed a general rate equation for silicate hydrolysis from transition state theory and irreversible thermodynamics. While their equation (1) like that of Dibble and Tiller (1981), "represents a completely general rate law it has many possible integrals, none of which is universally applicable to reactions among minerals and aqueous solutions" (Aagard and Helgeson, 1982) and a considerable amount of information is required about the reaction mechanism before this equation can be used. As this information is lacking, we have analyzed our data using Equations (3), (9), (10) and (11).

The temperature dependence of the rate constant can be described by the Arrhenius equation:

$$k_- = k'_- \exp\,(E_A/RT) \qquad (12)$$

where k'_- is a constant, E_A, the activation energy for precipitation, R, the gas constant and T, the temperature in degrees Kelvin. E_A can be calculated from the slope of a $\ln k_-$ vs 1/T plot assuming that the dissolution or precipitation mechanism does not change over the temperature range.

3. EXPERIMENTAL

3.1 Starting Materials

Natural quartz sands were used in all experiments.

Sand dissolution experiments were carried out on oil sand from the McMurray formation, from which the bitumen had been previously removed by soxhlet extraction with toluene. Small amounts of carbonaceous material that was not soluble in toluene were removed by dry sieving through a 32 mesh sieve, gravity separation in tetrabromoethane and hand picking. The cleaned sand consisted mainly of quartz, with very small amounts of kaolinite, illite and rutile, and contained 97% SiO_2 by weight. BET surface areas were measured on a Quantasorb® instrument. The results for eight one-gram sand samples ranged from 0.22 to 0.32 m^2/g with a mean of 0.26 ±0.03 m^2/g.

For the precipitation experiments it was necessary to use a coarser sand fraction to prevent fines transport and the 120-170 mesh fraction of an industrial quartz sand was selected. This sand was cleaned by ultrasonic vibration of small batches in tap water to loosen adhering fines. The water and suspended fines were decanted and the process was repeated until the water became clear. The sand was then washed twice with deionized water and dried. The cleaned sand contained 99% SiO_2 by weight. BET Quantasorb® surface areas of two duplicate samples were 0.0468 and 0.0473 m^2/g, equal within experimental error.

Dissolution experiments were conducted in deionized water and in 0.01 M borax solutions that had been brought to pH 6.5 and pH 7.5 by the addition of HCl. All precipitation experiments were carried out in deionized water.

3.2 Dissolution Experiments:

The dissolution experiments were carried out in 300 mL stainless steel autoclaves that were equipped with a sampling tube and valve (Figure 1A).

The sampling tube reached down to about 2 cm from the bottom of the autoclave. A 7 µm sintered stainless steel filter prevented fines from entering the tube. A weighed amount of cleaned Fort McMurray oil sand was put in the autoclave and approximately 200 mL of solution were added. The autoclave was then sealed and placed in a forced convection oven at the desired temperature. At regular intervals, the autoclave was taken from the oven and placed in an electric heating mantle that was kept at the same temperature as the oven.

A Quick Connect ® fitting was used to connect the sampling tube to a coiled stainless steel capillary tube immersed in ice, with a regulating valve at its end. Sampling valve and regulating valve were opened one after the other so that a steady flow of solution was obtained. The first 5 mL were discarded, and the next 5 mL were collected in sufficient cold deionized water to dilute the expected SiO_2 concentration to less than 100 ppm. The solution was adjusted to pH 2 with HNO_3 and was submitted for silica analysis.

Several autoclaves were placed in the oven simultaneously for each temperature. Samples were withdrawn periodically from an individual autoclave which resulted in a decrease in the mass of H_2O remaining. In most cases, sampling moved to another autoclave from the same experimental series after withdrawal of 3 to 4 samples. In this manner we were able to extend our runs to longer duration without having to account for large changes in the surface area to mass ratio.

Several experiments were conducted to measure the effect of changing the ratio of surface area of the sand to the mass of H_2O in the system. These experiments were run in the same autoclaves as the dissolution experiments described above. The ratio of sand to water was varied and sampling was carried out at a fixed time. k_- calculated from these experiments should be equal to k_- calculated from the experiments with time as a variable.

3.3 Precipitation Experiments:

The precipitation experiments were conducted in the flow-through system that is schematically represented in Figure 1B. The autoclaves were filled with the cleaned industrial quartz sand, sealed and flooded with deionized water using a positive displacement pump or a high pressure chromatography pump. The back-pressure regulator was set at 1-2 MPa above the saturated water vapor pressure at run temperature. The temperature in the oven was raised to a selected value in the range 250-275°C and kept at this level until the solution was saturated. The temperature was then lowered to the desired value while injecting water to maintain the pressure. When the temperature stabilized samples were taken at regular intervals by injecting water and withdrawing an equivalent amount of solution through the back-pressure regulator. The first 15 mL of sample were discarded and one or more samples ranging in size from 5 to 10 mL were collected. In this experimental design, the smaller vessel served as a buffer between the pump and the precipitation vessel. Calculations based on the assumption of plug flow showed that the deionized water injected during sampling never reached the bottom of the precipitation vessel and no dilution correction is required.

In Run #2, the "saturation" and "precipitation" vessels were put in separate ovens. At the start of the experiment, the solution in both vessels was saturated at 250°C, after which the temperature of the precipitation vessel was lowered to 155°C. Samples were taken from both vessels using the method described above.

3.4 Silica Analysis:

All samples from the dissolution experiments were analyzed by Atomic Absorption spectrometry (AAS) (Devine and Suhr, 1977). In the precipitation experiments, there was some difficulty in obtaining precise silica values by AAS so several different sampling procedures were tested and all samples were analyzed by both AAS and Inductively Coupled Plasma Spectrometery (ICP). In Experiment #2, single samples were collected in

sufficient deionized water to reach a final concentration of less than 100 ppm. In Experiments #3, 4 and 5, duplicate samples were collected in 0.05 M HCl. In Experiments #6, 7 and 8, one of the duplicate samples was collected in 0.05 M HCl and the other in 0.1 M NaOH. A number of samples were reanalyzed after a period of several weeks and no changes were observed.

Comparison of the analytical results showed that the ICP data are somewhat more precise than the AAS data and that 2.5% is a reasonable estimate of the relative standard deviation. A comparative study of the analytical results will be published elsewhere (Bird et al., in preparation).

3.5 Data Treatment:

The numerical results have been treated in a number of ways. For the dissolution experiments in which several samples were withdrawn from a single autoclave, we used Equation (9) in a modified form. The relationship between silica concentrations in sequential samples is given by:

$$\ln \left[\frac{C_{eq} - C_i}{C_{eq} - C_{i-1}} \right] = -(\Delta t / M_i)\, k_{-}\, A \qquad (13)$$

where C_i = SiO_2 concentration in sample i, taken at time t_i, $\Delta t = t_i - t_{i-1}$, M_i is the mass of water present during the period t, and C_{eq} is calculated from Equation (3).

A least squares fit of Equation (13) to the data gives a straight line with slope $k_{-}A$. Equation (13) however, cannot be used to calculate the error on the slope as subsequent values of the logarithmic terms are not independent. The concentration that appears in the numerator of one term appears in the denominator of the next. This means that a positive deviation from the "true value" for one data point automatically results in a negative deviation from the "true value" for the next data point and the calculated error in slope is too large. Since the deviations compensate for each other, the slope is still correct.

We also fitted Equation (10) to the dissolution data without making any correction for sample withdrawal using a weighted least squares linear regression procedure. In general it was found that the first few data points fell off the least squares regression lines and a considerably better fit could be obtained using an equation of the form:

$$-\ln [1 - C/C_{eq}] = k_- (A/M)\, t + B \qquad (14)$$

where B is a constant.

Putting $t = 0$, "C_o" $= C_{eq} (1 - \exp(-B))$ (14a)

It was found that the k_- values obtained from Equations (13) and (14) were equal within the error estimated from Equation (14) with the exception of Experiment 7 (Table 1). In this experiment, a large number of samples had been withdrawn from a single autoclave. It seems reasonable to assume then, that the experimental errors in k_- values found using Equation (13) are of the same order of magnitude as estimated by using the least squares regression on Equation (14). The k_- values reported in Table 1 were calculated using Equation (13) and the associated errors were calculated from Equation (14).

For the dissolution experiments in which A/M was varied at constant time $-\ln(1-C/C_{eq})$ was plotted as a function of A/M and the data were subjected to least squares linear regression analysis.

The precipitation data were analyzed with the aid of Equation (9).

Data from the non-linear portions of the curves were discarded and the weighted least square linear regression technique was used with the remaining data to calculate k_- and associated error.

Activation energies were obtained from Equation (12) for both the dissolution and precipitation experiments by a weighted least squares linear regression of log k_- on 1000/T (Equation 12). E_A and k' were calculated from the slope and y-intercept, respectively.

Kinetic equations of several different types were fitted to our data (see discussion in Lasaga, 1981), and in this report we will discuss the results obtained with an integrated form of Equation (11) with $\omega = -1/2$:

$$C = k_- (A/M)\, t^{1/2} \qquad (15)$$

4. RESULTS AND DISCUSSION

Sixteen dissolution experiments with time as the independent variable, seven precipitation experiments and four dissolution experiments with A/M as the independent variable were carried out. The experimental conditions and results of these runs are listed in Appendices I, II and III, respectively.

Equations (13) and (14) provided a good fit to the dissolution data. The results are given in Table 1. Equation (9) described the precipitation data well over most of the time range studied; for some runs, however, the data near the beginning and the end of the experiments deviated from the least squares regression line.

Higher-order equations did not describe either dissolution or precipitation data as well as did Equations (9), (13) and (14). However, Equation (15) gave as good a fit, and in some cases an even better fit than that obtained with (9), (13) and (14).

Figure 2 shows the results for dissolution experiment 4 as a typical example. In Figure 2A, Equation (14) was fitted to the data, in Figures 2B and 2C, Equations (13) and (15) were used, respectively.

The positive intercept with the vertical axis in Figure 2A has been observed by other authors (van Lier, 1960; Bergman, 1963; Henderson et al., 1970; Rimstidt and Barnes, 1980) who assumed that it was caused by rapid dissolution of a disturbed surface layer of high solubility. Moore and Rose (1975) thought that it resulted from the dissolution of very fine particles adhering to the quartz surface. In either case, "C_o" (Equation (14a)) is a measure of the amount of quartz dissolved during the initial rapid dissolution stage. To test this hypothesis, we reused the sand remaining from Experiments 6, 8, 10 and 12 in Experiments 7, 9, 11 and 13, respectively. As part of the disturbed surface layer should have been removed in the initial experiments, C_o should be smaller in the second experiment. For the three pairs, 6-7, 8-9 and 10-11 "C_o" was lower in the second experiment, which agrees with the hypothesis outlined above. However, the reverse occurred in the pair 12-13 where "C_o" was higher in the second experiment.

In our dissolution runs, we noted that the length of time over which the results agreed with Equation (15) changed with temperature. At 150°C, the parabolic region can last to several hundred hours, at 200°C this was reduced to 10 hours or less, and at 250°C, to 6 hours or less. In this context, it is important to note that a parabolic kinetic model cannot track the dissolution or precipitation process as it approaches equilibrium, and in this sense, the duration of the "parabolic kinetics" is in itself a function of the rate of approach to equilibrium and a parabolic rate law by itself can never provide a complete description of the process.

In the experiments of van Lier et al. (1960), the concentration of silica in solution followed a parabolic, linear or logarithmic time dependence depending on the ionic strength of the solution (see Dibble, 1980, Figure 2A and 2B). Similar observations have been made on the dissolution kinetics of other silicate systems and a number of models, none of which have been completely successful, have been put forward to rationalize these observations (Wollast, 1967; Lagache, 1976; Luce et al., 1972; Petrovic et al., 1976; Fung et al., 1980; Dibble and Tiller, 1981; Aagard and Helgeson, 1982 and others).

Table 1 summarises the results of our dissolution experiments and lists k_- values and associated errors as calculated from Equations (13) and (10), respectively.

The results of our precipitation experiments are given in Table 2 which summarises the experimental conditions, the rate constants k_- and associated errors as calculated from Equations (3) and (9). Figure 3A shows a plot of the data for Run #3 (Table 2) using Equation (9). Figure 3B shows the same experimental data using Equation (15). The goodness of fit using Equations (9) and (15) is nearly identical for the two cases.

The only other precipitation data for quartz available in the literature are those of Rimstidt (1979). For comparison, we analyzed his raw data in exactly the same way as we analyzed ours. Figure 4A shows Rimstidt's Runs

2E and 2F calculated using Equation (3) and (9) and (3) and (10), respectively. This figure is effectively identical to Figure 3 in Rimstidt and Barnes (1980). Figure 4B shows the same data as 4A with Equation (15) fitted to the data. A straight statistical comparison shows that the equations used in 4A and 4B are equally good as a linear representation of the data, and points which deviate from the line in 4A also deviate from the line in 4B.

Although parabolic dissolution behavior has been discussed widely in the geochemical literature, only one other example of a parabolic precipitation rate has been reported. Holdren and Adams (1982) showed that co-precipitation of aluminosilicate minerals and quartz could account for the observed change in the silica concentration with time. It seems unlikely however, that this mechanism is responsible for the results reported here where the parabolic time dependence occurred over a wide range of experimental conditions using a variety of reaction materials of varying degrees of purity.

It is not possible to account for the parabolic time dependence through a reaction of a disturbed surface layer or attached fines. The dissolution experiments were carried out for long periods of time and any disturbed surface layer would have dissolved very early on in the experiment. In the precipitation experiments, the sand was initially reacted for several tens of hours at a higher temperature than that used for precipitation. This pre-equilibration step should have removed any disturbed surface layer before the precipitation was initiated.

At this time, we have no satisfactory theoretical explanation for the parabolic time dependence.

In four experiments, time was fixed and A/M was the independent variable. Figure 5 shows a plot of $-\ln (1-C/C_{eq})$ versus A/M for the experiment at 205°C where samples were taken after 21 hours (Equation (10) with t fixed and A/M variable). The data plot as a distinct curve which can be resolved into two linear segments with different slopes. For Run 1A, the slope of

the segment with A/M ratios between 1.3 and 15.7 m^2/kg corresponds to $k_- = 3.3 \times 10^{-7}$ sec^{-1} whereas the slope of the segment with A/M ratios between 17.4 and 39.2 m^2/kg (Run 1B), corresponds to $k_- = 9.5 \times 10^{-8}$ sec^{-1}. The other three experiments (Table 3) showed a similar trend; k_- is smaller at higher A/M ratios and larger at lower A/M ratios.

The decrease in k_- with increasing values of A/M is possibly due to the way the dissolution experiments were conducted. Samples were taken from the bulk fluid just above the sand. The pore fluid in the sand equilibrates with the bulk fluid by diffusion of dissolved silica. The diffusion path is tortuous, the cross section for diffusion is small and concentration gradients along the path get smaller with increasing distance from the sand/bulk solution interface. With increasing A/M, diffusion from the deepest sand layers probably becomes slower than dissolution, and the bulk solution concentration increases more slowly than predicted by Equation (10). These observations suggest that pore geometry and diffusion may be important in controlling the rate of transport from the dissolving silica grains to the bulk solution.

Most of our dissolution experiments were carried out at an A/M of 5.2 m^2/kg where Equation (10) applies. Experiments 2, 3, 4 and 5 (Table 1) fall somewhat beyond the range where Equation (10) is valid and k_- derived for these experiments may be too low.

In the precipitation experiments, the pore solution was sampled directly and diffusion rates should not have affected the silica concentration in the fluid.

Rimstidt (1979) reported experiments carried out by Usdowski in which A/M was varied. Five samples with A/M between 0.173 and 1.36 m^2/kg were reacted at 173°C, 202°C and 223°C, presumably in static autoclaves. Figure 6A shows a logarithmic plot of Usdowski's data at 173°C and his rate constant data are plotted against A/M in Figure 6B. As in our experiments, the dissolution rate decreased with increasing A/M.

The activation energy for precipitation and the pre-exponential constant k' were determined from an Arrhenius plot (Equation (11)). Our data (from Tables 1 and 2) are plotted in Figure 7, together with those of Rimstidt and Barnes (1980) and van Lier et al. (1960). Usdowski's results were not included on the figure because they plot well away from the major trend in Figure 7 and we suspect some inconsistency in effective surface area. Also, the k_- values we calculated from Usdowski's data were four times greater than those calculated by Rimstidt from the same data. We also corrected the k_- values of Rimstidt's points 2M and 20 (1979) as there was a mistake in his calculations.

The data on Figure 7 occur in clusters corresponding to precipitation, dissolution or investigators. Within each set, there is considerable scatter and an even greater scatter between the different sets.

Activation energies, values of the pre-exponential constant and error estimates for each set of data were obtained by linear regression and are listed in Table 4. The experimental error in both the activation enery and the pre-exponential term k' is very large and there is no statistically significant difference between the values from the various sets. However, the clustering of data points suggests that there are systematic differences between the groups and that the data from different experimental systems should not be combined. In fact, combination of all data results in an activation energy of 78 KJ/mole which is much larger than that for any of the individual sets (see Table 4).

An Arrhenius plot of our parabolic rate constants (see Equation (15)) resulted in an activation energy for precipitation of 62 K joules $mole^{-1}$, which is equal, within the error, to that obtained from the first order rate law.

Errors in measuring surface area may contribute to spread within and between the data reported by different investigators. The BET method for estimating surface area is not particularly accurate for the low surface areas used by all investigators. A systematic error in estimating surface

area would not appear if only one starting material were used in an individual set of experiments but will appear when the results of different investigators are compared.

The activation energies from our dissolution experiments and Rimstidt's are equal within experimental error. The activation energies from the precipitation experiments seem to be smaller than those from dissolution, even though the large experimental error makes it difficult to draw a definite conclusion and more experiments would be needed to verify this observation. We have not been able to suggest a possible cause for such a difference but speculate that effective surface area in the experiments may differ from the measured surface area.

At this time it is impossible to specify a detailed reaction mechanism in terms of either the quartz surface or the silica species present in solution. The similarity between the dissolution behavior of quartz and other silicates and the high activation energies of dissolution and precipitation suggest that reaction of the Si-O framework is probably the most important aspect of silica and silicate dissolution reactions. This reaction is complex and depends on a number of variables including surface charge, ionic strength of the solution, temperature, pressure, etc. It almost certainly proceeds through several steps.

Much more detailed experimention is needed to develop a mechanistic kinetic model for quartz dissolution. However, the activation energies and pre-exponential terms listed in Table 4 can be used to calculate a rate constant for any temperature (Equation 12). Together with Equation (9), they are very useful in the prediction of silica mass transport during steam injection into oil sands, as will be shown in the second paper of this series (Boon, Bird and Stone, in preparation).

No data on the dissolution and precipitation behavior of quartz at high temperature, as a function of salinity or pH (at pH > 7.5) are now available. Further studies in this area would extend the range over which mass transport predictions can be made.

5. SUMMARY AND CONCLUSIONS

Nineteen dissolution and seven precipitation experiments were carried out at temperatures between 121°C and 250°C and corresponding water vapor pressure. The results of the dissolution experiments are in reasonable agreement with those reported previously by van Lier et al. (1960), Rimstidt (1979) and Rimstidt and Barnes (1980) and can be described by a zero-order dissolution, first order precipitation reaction. The activation energy for quartz precipitation lies between 51 to 55 kJ $mole^{-1}$. The activation energy obtained from our precipitation experiments was somewhat smaller but the difference is not statistically significant.

Most of the data, particularly below 200°C, can also be described by a parabolic rate equation, which leads to an activation energy in the same range as that found above. The high activation energy suggests that disruption of the Si-O framework is the rate-determining step.

For the experiments in which the ratio (surface area of quartz)/(mass of H_2O) was the independent variable, we found that the rate constants obtained at high A/M are smaller than those obtained at low A/M. It was shown that this may have been caused by the experimental set-up, in which diffusion from pore solution to bulk solution may become the rate-determining step at high A/M.

The zero-order-first order equation can be used to predict silica mass transport during steam injection.

6. REFERENCES

Aagard, P. and Helgeson, H.C. (1982). Thermodynamic and kinetic constrainsts on reaction rates among minerals and aqueous solutions. I. Theoretical considerations. A. J. Sci., 282:237-285.

Bergman, I. (1963). Silica powders of respirable size. III. Dialysis of quartz powders against dilute sodium hydroxide. J. Appl. Chem. 13:319-323.

Crerar, D.A. and Anderson, G.M. (1971). Solubility and solvation reactions of quartz in dilute hydrothermal solutions. Chem. Geol., 8:107-122.

Devine, J.C. and Suhr, N.H. (1977). Determination of silicon in water samples. Atomic Abs. Newsletter, 16:39-41.

Dibble, W.E. Jr. (1980). Non-equilibrium water/rock interactions. Ph.D. Dissertation, Stanford University, Stanford, California.

Dibble, W.E. Jr. and Tiller, W.A., (1981). Non-equilibrium water/rock interactions - I. Model for interface - controlled reactions. Geochem. Cosmochim. Acta, 45:79-92.

Fleming, B.A. and Crerar, D.A. (1982). Silica acid ionization and calculation of silica solubility at elevated temeprature and pH. Application to geothermal fluid processing and reinjection. Geothermics, 11:15-29.

Fournier, R.O. and Potter, R.W. II. (1982). An equation correlating the solubility of quartz in water from 25° and 900°C at pressures up to 10,000 bars. Geochim. Cosmochim. Acta, 46:1969-1973.

Fung, P.C., Bird, G.W. McIntyre, N.S. and Sanipelli, G.G. (1980). Aspects of feldspar dissolution. Nuclear Techn., 51:188-196.

Helgeson, H.L. (1971). Kinetics of mass transfer among silicates and aqueous solutions. Geochim. Cosmochim. Acta, 35:421-469.

Henderson, J.H., Syers, J.K. and Jackson, M.L. (1970). Quartz dissolution as influenced by pH and the presence of a disturbed surface layer. Israel J. Chem., 8:357-372.

Holdren, G.R. and Adams, J.E. (1982). Parabolic dissolution kinetics of silicate minerals: An artifact of non-equilibrium precipitation processes. Geology, 10:186-190.

Lagache, M. (1976). New data on the kinetics of the dissolution of alkali feldspar at 200°C in carbon dioxide charged water. Geochim. Cosmochim. Acta, 40:157-161.

Lasaga, A.C. (1981). Rate laws of chemical reactions. In: A.C. Lasaga and R.J. Kirkpatrick (Editors), Kinetics of Geochemical Processes, Reviews in Mineralogy, 9. Min. Soc. Am. pp. 1-67.

Luce, R.W., Bartlett, R.W. and Parks, G.A. (1972). Dissolution kinetics of magnesium silicates. Geochim. Cosmochim. Acta, 26:35-50.

McCorriston, L.L., Demby R.A. and Pease, E.C. (1981). Study of reservoir damage produced in heavy oil formations due to steam injection. Society. Pet. Eng. preprint SPE 10077, presented at 56th annual fall tech. conference, San Antonio, Texas, October 1981.

Moore, G.S.M. and Rose, H.E. (1975). Dissolution of powdered quartz. Nature, 253:525-527.

Petrovic, R. (1976). Rate control in feldspar dissolution - II. The protective effects of precipitates. Geochim. Cosmochim. Acta, 40:1509-1521.

Reed, M.G. (1979). Gravel pack and formation sandstone dissolution during steam injection. Society of Pet. Eng. preprint SPE 8424, presented at the 54th annual technical meeting, Las Vegas, September 1979.

Rimstidt, J.D. (1979). The kinetics of silica-water reactions. Ph.D. thesis, Pennsylvania State University, University Park, Pennsylvania.

Rimstidt, J.D. and Barnes, H.L. (1980). The kinetics of silica-water reactions. Geochim. Cosmochim. Acta, 44:1683-1699.

Van Lier, J.A., De Bruyn, P.L. and Overbeek, J. Th. G. (1960). The solubility of quartz. J. Phys. Chem., 64:1675-1682.

Walther, J.V. and Helgeson, H.C. (1977). Calculation of the thermodynamic properties of aqueous silica and the solubility of quartz and its polymorphs at high pressures and temperatures. A. J. Sci., 277:1315-1351.

Wollast, R. (1967). Kinetics of alteration of K-feldspar in buffered solutions at low temperature. Geochim. Cosmochim. Acta, 31:635-648.

ACKNOWLEDGEMENTS

This work was carried out as part of the Hydrothermal Chemistry Project in the Oil Sands Research Department of the Alberta Research Council. Financial support was provided by the Alberta Research Council/Alberta Oil Sands Technology and Research Authority Joint Oil Sands Research Program.

Our colleagues, W.D. Gunter and Peter Tremaine provided many constructive suggestions during the experimental phase of the work and on the manuscript. Brian Wiwchar, Larry Holloway and Shawn Cake carried out most of the experimental work. Larry Holloway and Brian Fuhr of Oil Sands Analytical Services spent many hours on the silica analyses and even more hours discussing the results. Diane Teppan and Phyllis Kozak were responsible for turning our illegible scribbles into a completed manuscript. We gratefully acknowledge all of these contributions.

TABLE 1
DISSOLUTION KINETIC RUN RESULTS

Run #	Temperature °C	Run Duration (Hours)	Number of Samples Taken	A/M (m^2 kg^{-1})	k_- (sec^{-1})	2σ k_- (sec^{-1})
3 Deionized H_2O	150	668	6	17.3	4.11×10^{-8}	4.1×10^{-8}
4 " "	170	120	6	17.3	6.47×10^{-8}	7.6×10^{-8}
5 " "	205	1,027	9	17.3	1.63×10^{-7}	9.4×10^{-8}
6 " "	252	288	7	17.3	4.40×10^{-7}	1.5×10^{-7}
7 " "	250	48	7	5.2	1.83×10^{-6}	1.0×10^{-6}
8 " "	200	500	11	5.2	2.68×10^{-7}	1.1×10^{-7}
9 " "	200	646	10	5.2	1.51×10^{-7}	1.8×10^{-7}
10 " "	250	338	7	5.2	7.29×10^{-7}	4.2×10^{-7}
11 " "	250	513	14	5.2	1.08×10^{-6}	3.1×10^{-7}
12 " "	250	48	13	5.2	2.34×10^{-6}	4.8×10^{-7}
13 " "	255	24	6	5.2	1.27×10^{-6}	6.0×10^{-7}
14 " "	255	48	11	5.2	1.68×10^{-6}	3.0×10^{-7}
15 pH 6.5	200	507	11	5.2	2.62×10^{-7}	1.2×10^{-7}
16 pH 6.5	250	432	10	5.2	8.25×10^{-7}	2.0×10^{-7}
17 pH 7.5	200	454	10	5.2	2.91×10^{-7}	1.2×10^{-7}
18 pH 7.5	250	336	11	5.2	5.17×10^{-7}	1.5×10^{-7}

Table 1: Dissolution kinetic run results. Complete tables of the actual experimental data are given in Appendix I.

TABLE 2
PRECIPITATION KINETIC RUN RESULTS

Run #	Saturation T(°C)	Precipitation T(°C)	Run Duration (Hours)	Number of Number of Data Points	A/M (m^2 kg^{-1})	k_- (sec^{-1})	2σ k_- (sec^{-1})
2	250	155	1,042	27	140	9.9×10^{-10}	2.8×10^{-10}
3	265	177	217	11	156	6.5×10^{-9}	1.4×10^{-9}
4	265	177	113	8 duplicate	124	7.6×10^{-9}	3.0×10^{-9}
5	265	200	210	15 duplicate	209	1.7×10^{-8}	5.2×10^{-9}
6	271	155	266	14 duplicate	116	1.3×10^{-8}	1.4×10^{-9}
7	271	221	266	13 duplicate	177	2.5×10^{-8}	1.6×10^{-8}
8	275	123	512	12 duplicate	156	2.8×10^{-9}	6.2×10^{-10}

Table 2: Precipitation kinetic run results. Complete tables of the actual experimental data are given in Appendix II.

TABLE 3

Experiment #	Temperature (°C)	Time (hours)	A/M range (m^2 kg^{-1}) min	A/M range (m^2 kg^{-1}) max	k_- (sec^{-1})
1a	205	21	1.3	15.66	3.3×10^{-7}
1b	205	21	17.41	39.2	9.48×10^{-8}
2a	200	40.5	0.52	1.30	6.73×10^{-7}
2b	200	40.5	3.91	6.25	1.30×10^{-7}
3a	250	21	0.13	2.61	2.03×10^{-6}
3b	250	21	5.22	26.1	6.28×10^{-7}
4a	250	40.5	2.61	7.83	6.67×10^{-7}
4b	250	40.5	7.83	26.1	8.09×10^{-7}

Table 3: Experiments with A/M as the independent variable. Each A/M range used to obtain k_- is defined by its minimum and maximum value. See text for explanation. Complete tables of the actual experimental data are given in Appendix III.

TABLE 4
CALCULATED ACTIVATION ENERGY FOR PRECIPITATION (E_A)
FOR VARIOUS EXPERIMENTAL CONDITIONS

Experiments	Number of Data Points	E_A kJ/mole	$2\ E_A$	log k_'	2σ log k_'
Rimstidt (1979) Dissolution Experiments	6	55.1	7.6	-0.42	8.34
Rimstidt (1979) Precipitation Experiments	5	41.7	11.9	-2.18	1.48
Rimstidt (1979) Combined Dissolution & Precipitation	11	60.5	6.1	-0.35	0.76
This Report Dissolution Experiments	16	51.4	14.7	0.47	1.36
This Report Dissolution Experiments with A/M = 17.4 m^2/kg	4	43.3	23.3	-2.03	2.27
This Report Precipitation Experiments	7	34.3	10.3	4.19	1.26
Combined Data, This Report & Rimstidt (1979)*	34	78.3	6.1	1.68	0.36
Usdowski (1979)* Dissolution	15	75.4	13.6	2.67	1.50

* Usdowski's data were not included in the combined data set for reasons discussed in text.

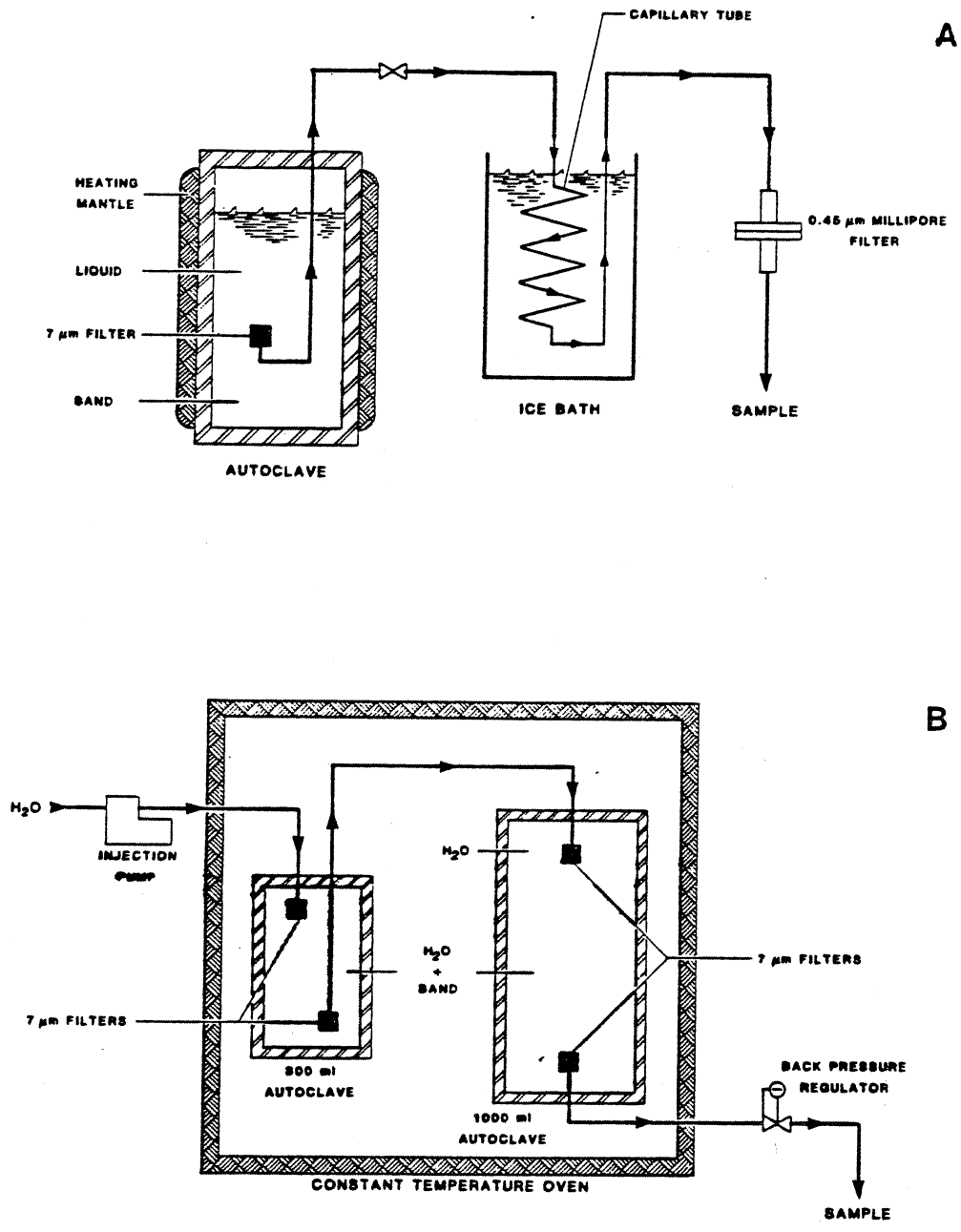

Figure 1 A. Apparatus used in the dissolution and A/M experiments.

B. Flow system used for the precipitation experiments.

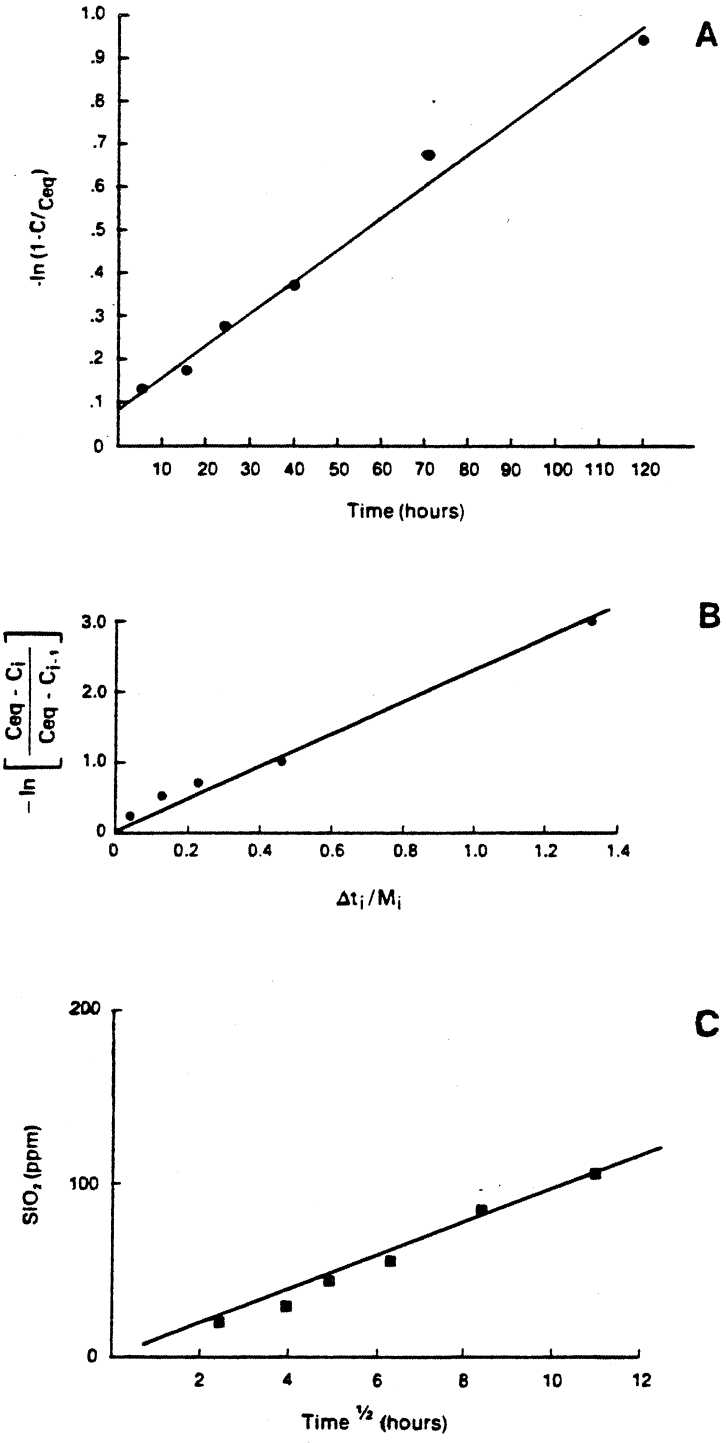

Figure 2 A. Plot of $-\ln(1 - C/C_{eq})$ versus time for Experiment 4, Table 1 (Equation 14).

B. Plot of $-\ln[(C_{eq} - C_i)/(C_{eq} - C_{i-1})$ versus $\Delta t_i/M_i$ for Experiment 4, Table 1 (Equation 13). See Text for discussion.

C. Silica concentration versus $t^{1/2}$ for Experiment 4, Table 1 (Equation 15). See text for discussion.

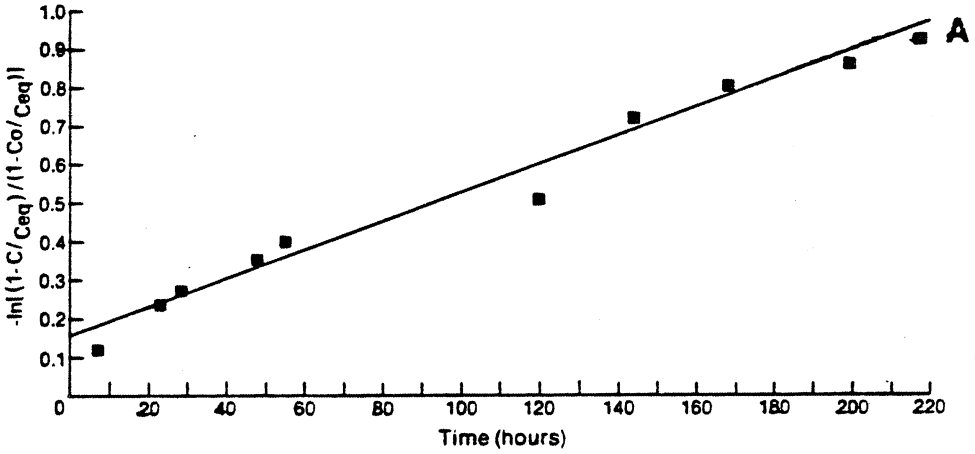

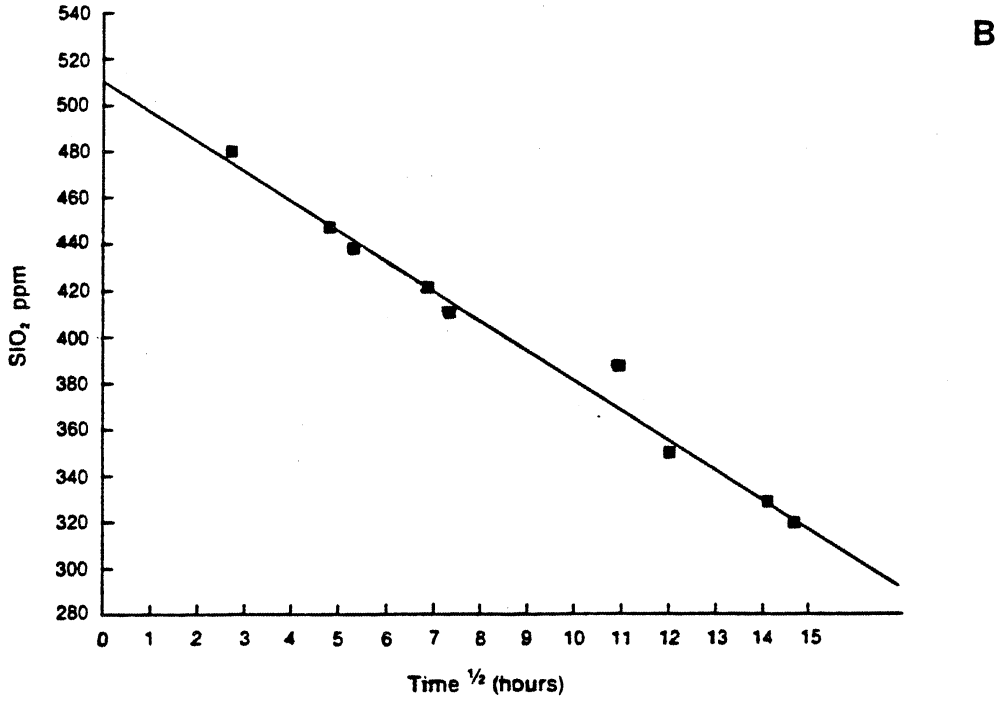

Figure 3 A. A first order rate constant plot for precipitation - Run 3, (Table 2) at 177°C (Equation 9).

B. The silica concentration for Run 3 plotted against $t^{1/2}$ (Equation 15).

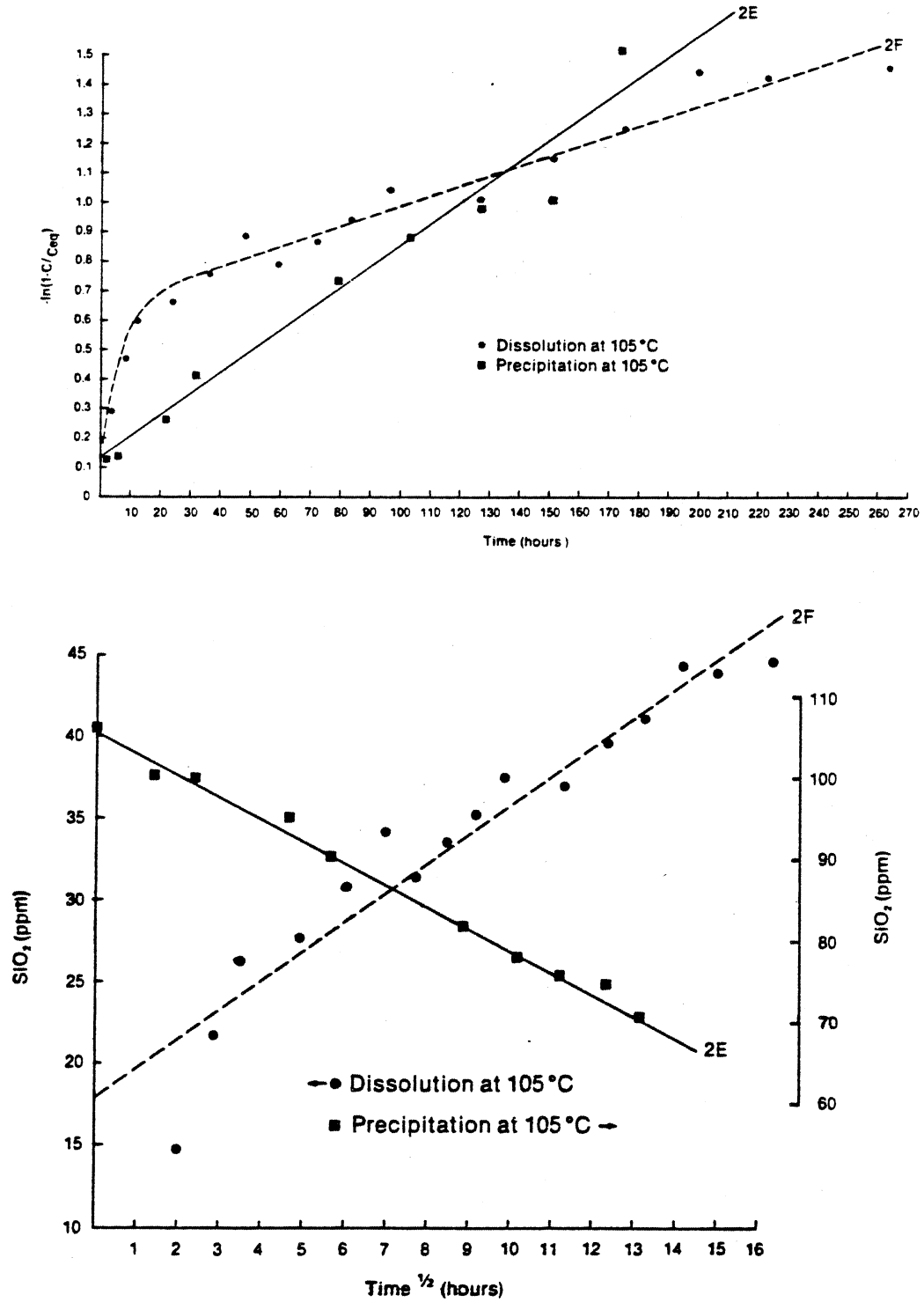

Figure 4 A. Dissolution and precipitation Runs 2E and 2F of Rimstidt (1979) plotted using first order rate constant model (Equations 9 and 10).

B. Rimstidt's Run 2E and 2F data plotted using Equation (15).

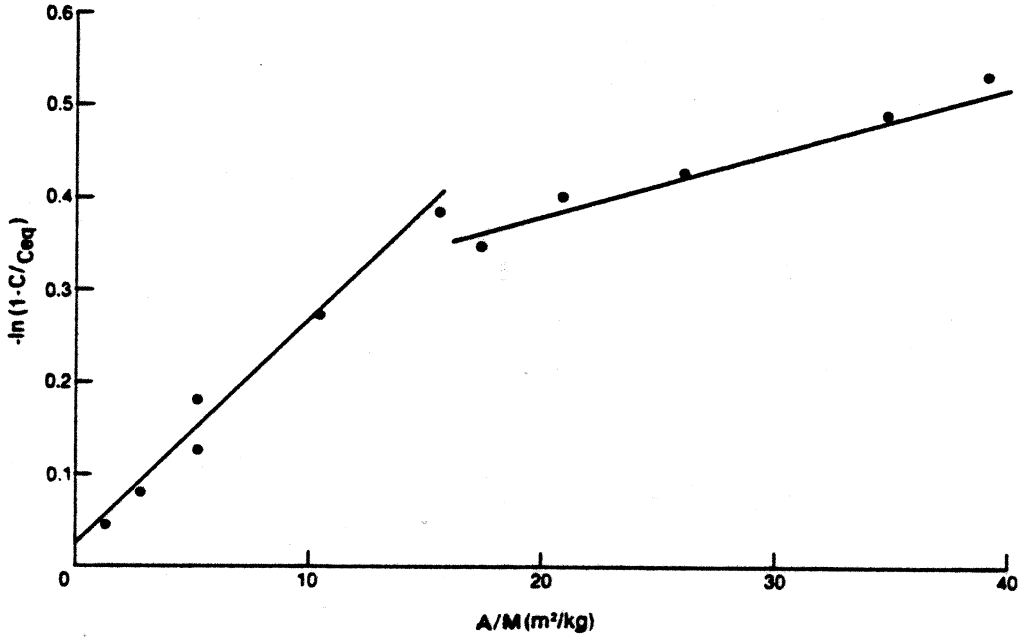

Figure 5 -ln (1 - C/C_{eq}) versus A/M at 205°C. Samples were taken after 21 hours. The parameters calculated for the two linear segments are listed in Table 3.

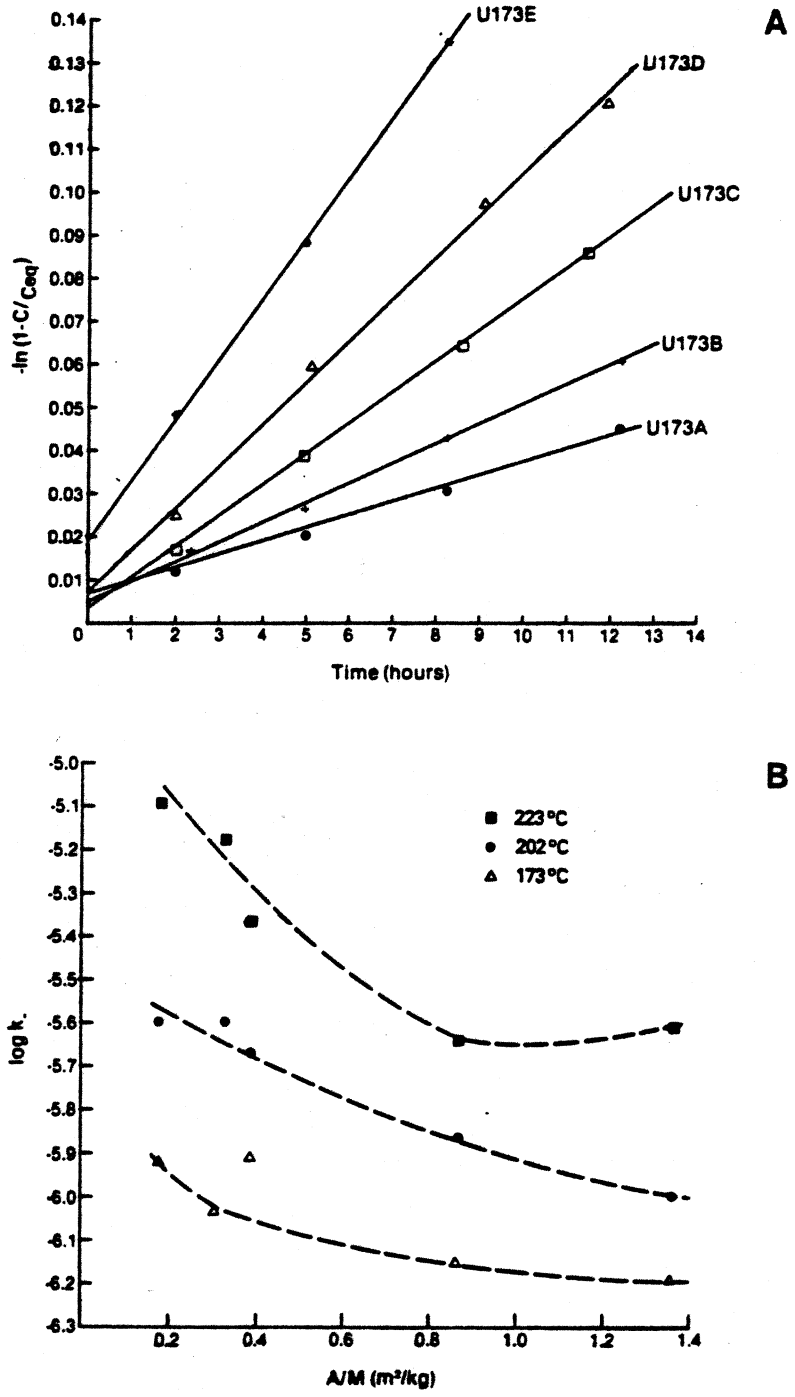

Figure 6 A. $-\ln (1 - C/C_{eq})$ versus time for Usdowski's 173°C dissolution experiments for five different values of A/M.

B. Log k_- versus A/M for the five experiments shown in 6A. Data plotted are those reported in Rimstidt (1979). While our recalculation of these data leads to rate constants which are larger by a factor of 4, the trend in the data is unchanged and the factor of 4 only shifts the individual lines to higher values on the vertical axis.

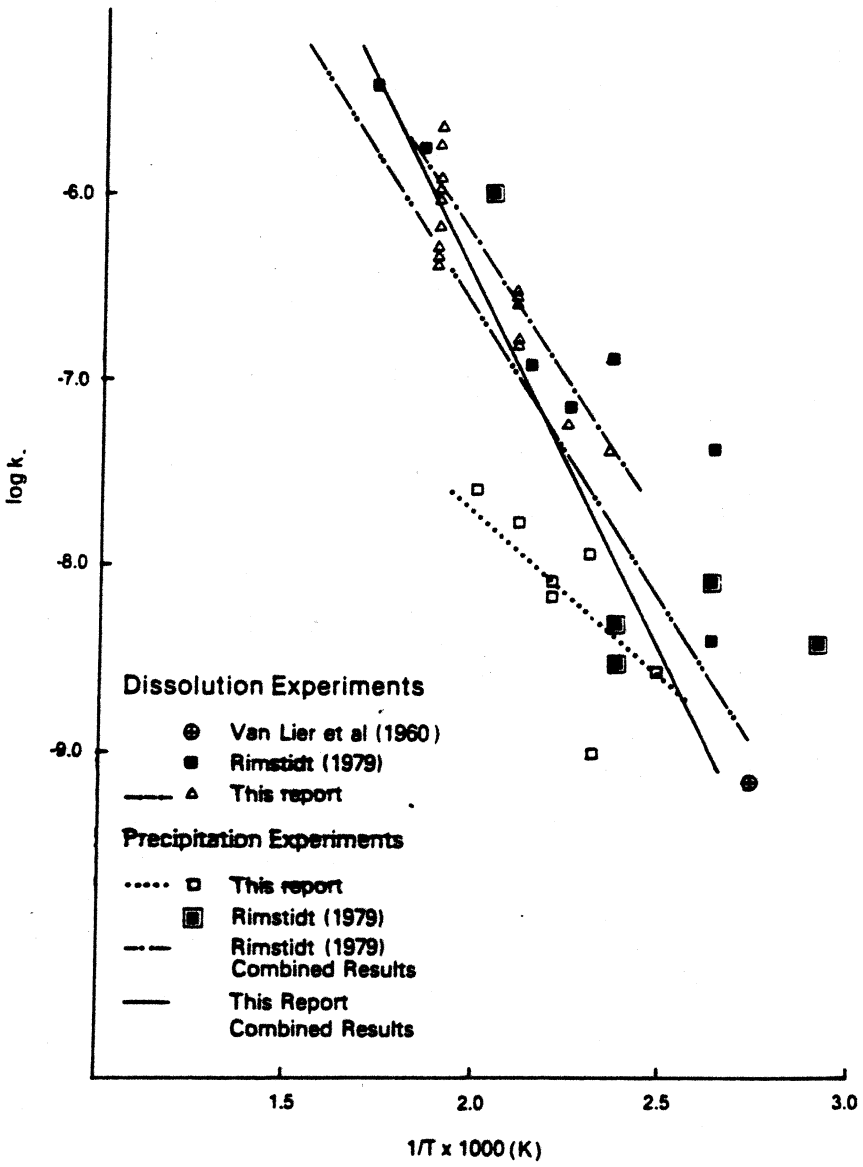

Figure 7 Arrhenius plot of our dissolution and precipitation experiments (Table 1 and 2), and those of Rimstidt (1979) and Van Lier et al. (1960). Usdowski's data were not plotted for the reason discussed in the text. Regression lines are shown for our dissolution and precipitation results and Rimstidt's combined data. Constants for these lines are listed in Table 4.

- APPENDIX I -

EXPERIMENTAL RESULTS FOR QUARTZ DISSOLUTION RUNS

RUN #3
150°C 17.3 m^2/kg
Deionized Water

Time of Sampling (Hours)	ppm SiO_2
21	21
46	43
143	66
239	73
499	107
668	124

RUN #4
170°C 17.3 m^2/kg
Deionized Water

Time of Sampling (Hours)	ppm SiO_2
5.5	21
16.0	28
24.0	43
40.0	54
71.0	86
120.0	107

RUN #5
205°C 17.3 m^2/kg
Deionized Water

Time of Sampling (Hours)	ppm SiO_2
24	107
24	113
72	171
96	235
96	223
213	270
525	263
935	270
1,027	270

RUN #6
252°C 17.3 m^2/kg
Deionized Water

Time of Sampling (Hours)	ppm SiO_2
3.5	182
8.0	212
20.0	286
29.5	323
45.0	349
72.0	377
288	415

RUN #7
250°C 5.2 m^2/kg
Deionized Water

Time of Sampling (Hours)	ppm SiO_2
2.0	56
3.7	90
6.0	142
8.0	176
24	344
32.4	385
48.0	415

RUN #8
200°C 5.2 m^2/kg
Deionized Water

Time of Sampling (Hours)	ppm SiO_2
6	64
23	88
47	109
75	126
94	150
166	193
214	210
334	235
380	235
428	240
500	248

RUN #9
200°C 5.2 m^2/kg
Deionized Water

Time of Sampling (Hours)	ppm SiO_2
6	28
24	58
48	92
71	156
143	195
167	212
215	246
311	256
365	255
646	256

RUN #10
250°C 5.2 m^2/kg
Deionized Water

Time of Sampling (Hours)	ppm SiO_2
19	220
43.5	285
67.0	342
163	398
235	409
331	409
338	415

RUN #11
250°C 5.2 m^2/kg
Deionized Water

Time of Sampling (Hours)	ppm SiO_2
4.5	111
22.5	246
47.0	285
73.0	342
122	415
170	415
193	415
238	415
238	415
267	415
340	415
361	415
465	415
513	415

RUN #12
250°C 5.2 m^2/kg
Deionized Water

Time of Sampling (Hours)	ppm SiO_2
2	64
4	79
6	125
8	155
18	229
19	226
24	319
24	323
28	343
32	350
40	380
44	390
48	407

RUN #13
255°C 5.2 m^2/kg
Deionized Water

Time of Sampling (Hours)	ppm SiO_2
2.0	86
4.0	118
6	128
8	168
16	220
24	300

RUN #14
255°C 5.2 m^2/kg
Deionized Water

Time of Sampling (Hours)	ppm SiO_2
2	49
4	58
6	83
8	111
16	212
20	249
24	278
32	321
40	343
48	367
48	360

RUN #15
200°C pH 6.5 5.2 m^2/kg

Time of Sampling (Hours)	ppm SiO_2
16	49
30	107
48	135
76	135
95	182
172	186
215	220
340	235
387	238
421	246
507	242

RUN #16
250°C pH 6.5 5.2 m^2/kg

Time of Sampling (Hours)	ppm SiO_2
4	94
24	246
48	287
72	332
96	340
144	415
192	362
240	402
288	415
338	402
432	415

RUN #17
200°C pH 7.5 5.2 m^2/kg

Time of Sampling (Hours)	ppm SiO_2
6	62
16	86
46	163
48	124
118	186
166	199
208	214
286	227
333	238
454	240

RUN #18
250°C pH 7.5 5.2 m^2/kg

Time of Sampling (Hours)	ppm SiO_2
6.0	158
16	173
30	227
48	276
76	312
95	327
167	363
215	364
215	415
336	404

- APPENDIX II -

EXPERIMENTAL RESULTS FOR QUARTZ

PRECIPITATION RUNS

TABLE A2-1
Run 2: 155°C

Sample #	PPm SiO_2		Run Duration (Hours)
	AA*	ICP**	
5	400	390	2
7	389	na	4
9	394	384	6
13	427	392	7.5
17	407	382	24
17a	356	na	24
23	364	384	30
27	368	386	48
31	368	386	54
35	367	380	97
39	379	375	124
45	330	367	147
45a	335	na	147
49	343	361	167
53	330	367	207
57	319	na	277
61	354	354	301
65	346	346	324
69	342	347	348
73	340	336	372
79	342	na	444
81	321	330	468
85	296	323	492
89	295	317	517
93	295	323	541
97	298	317	631
101	302	316	654
105	305	314	685
109	309	313	755
113	285	308	802
117	280	325	876
121	283	317	966
125	277	319	1,042

*AA = Atomic Absorption
**ICP = Inductively Coupled Plasma
na = not analyzed

TABLE A2-2
Run 3: 177°C

Sample #	PPm SiO_2		Run Duration (Hours)
	AA	ICP	
48	422	512	0
52	482	555	0
56	433	524	0
58	433	515	0
60	426	512	0
62	388	480	7
66	349	448	23
70	355	439	28
74	376	421	48
78	367	410	55
84	336	388	120
88	330	350	144
131	316	339	168
137	319	330	199
3	300	320	217
5	289	319	217
7	290	321	217

TABLE A2-3
Run 4: 177°C

Sample #	PPm SiO_2		Run Duration (Hours)
	AA	ICP	
21	532	492	0
22	560	493	0
23	482	432	5
24	497	424	5
26	447	396	18
27	441	386	18
30	420	387	42
31	394	368	42
34	413	389	48.5
35	408	377	48.5
38	399	354	65
39	393	378	65
40	393	351	89
41	385	348	89
44	378	350	96.5
45	380	343	96.5
48	322	315	113
49	277	323	113

TABLE A2-4
Run 5: 200°C

Sample #	PPm SiO_2		Run Duration (Hours)
	AA	ICP	
0	526	430	0
1	531	439	0
2	543	438	0
3	505	417	0
4	524	427	0
5	482	400	4.25
6	484	400	4.25
7	445	392	7.3
8	455	384	7.3
9	422	365	23
10	393	359	23
11	426	351	30.5
12	413	349	30.5
13	399	343	47.5
14	410	337	47.5
15	376	329	55
16	393	333	55
17	360	306	78.5
18	338	303	78.5
19	328	297	94.5
20	329	309	94.5
28	332	287	128
29	342	296	128
32	319	292	152
33	325	293	152
36	339	299	158
37	334	298	158
42	310	307	203
43	323	307	203
46	321	289	210
47	322	320	210

TABLE A2-5
Run 6: 155°C

Sample #	PPm SiO_2		Run Duration (Hours)
	AA	ICP	
A9	492	541	0
B9	509	563	0
A11	430	500	0
B11	499	503	0
A13	383	446	6.5
B13	404	459	6.5
A15	387	436	30.5
B15	392	428	30.5
A17	381	439	36.5
B17	385	429	36.5
A19	375	423	59.5
B19	381	414	59.5
A21	351	394	65.5
B21	358	391	65.5
A23	319	369	89.5
B23	329	356	89.5
A25	298	331	95.5
B25	311	333	95.5
A27	242	280	191.5
B27	251	267	191.5
A29	223	252	215.5
B29	250	272	215.5
A31	222	251	242
B31	227	241	242
A33	198	199	266
B33	194	206	266
A35	201	199	362
B35	214	206	362

TABLE A2-6
Run 7: 221°C

Sample #	PPm SiO_2		Run Duration (Hours)
	AA	ICP	
A8	411	460	0
B8	411	460	0
A12	499	570	0
B12	507	573	0
A14	445	503	6.5
B14	439	503	6.5
A16	392	450	30.5
B16	402	450	30.5
A18	381	436	36.5
B18	392	439	36.5
A20	377	416	59.5
B20	391	428	59.5
A22	373	416	65.5
B22	380	418	65.5
A24	361	409	89.5
B24	375	418	89.5
A26	362	404	95.5
B26	370	409	95.5
A28	351	399	191.5
B28	368	417	191.5
A30	348	396	215.5
B30	357	406	215.5
A32	344	408	242
B32	356	410	242
A34	327	327	266
B34	339	349	266

END OF RUN

TABLE A2-7
Run 8: 123°C

Sample #	PPm SiO_2		Run Duration (Hours)
	AA	ICP	
A36	521	534	0
B36	553	558	0
A38	550	553	0
B38	546	546	0
A40	503	525	2
B40	508	517	2
A41	469	489	6
B41	533	539	6
A42	430	418	24
B42	537	508	24
A43	427	417	30.5
B43	461	423	30.5
A44	419	419	54.5
B44	435	425	54.5
A45	423	423	62.5
B45	447	425	62.5
A46	418	413	78.5
B46	443	426	78.5
A47	400	395	178
B47	407	420	178
A48	375	380	230
B48	381	375	230
A49	352	325	272
B49	367	336	272
A50	326	315	344
B50	333	301	344
A51	296	289	416
B51	305	300	416
A52	274	269	512
B52	268	257	512

- APPENDIX III -

EXPERIMENTAL RESULTS FOR SURFACE AREA TO MASS OF WATER EXPERIMENTS

TABLE A3-1

205°C - 20 Hours Duration

A/M (m^2/kg)	SiO_2 Content (ppm)
0.13	6
0.26	6
0.65	6
1.30	13
2.61	21
5.22	32
5.22	43
8.35	64
10.44	65
15.66	87
17.41	80
20.9	90
26.1	94
34.8	97
39.2	112

TABLE A3-2

200°C - 40 Hours Duration

A/M (m^2/kg)	SiO_2 Content (ppm)
0.05	4.0
0.13	6.0
0.13	3.2
0.26	9.0
0.26	32
0.65	47
1.30	41
2.61	60
3.92	68
5.22	73
6.52	77

TABLE A3-3

250°C - 21 Hours Duration

A/M (m^2/kg)	SiO_2 Content (ppm)
0.13	13
0.26	24
0.65	56
1.30	81
2.61	116
2.61	143
5.22	165
5.22	177
7.83	203
10.4	203
13.05	245
19.6	297
26.1	322

TABLE A3-4

250°C - 40.5 Hours Duration

A/M (m^2/kg)	SiO_2 Content (ppm)
2.61	193
5.22	225
7.83	265
10.4	272
13.1	304
19.6	392
26.1	392